2021 43rd Annual International Conference of the
IEEE Engineering in Medicine & Biology Society (EMBC)
Oct 31 - Nov 4, 2021. Virtual Conference

Computational modeling of atherosclerotic plaque progression in carotid lesions with moderate degree of stenosis*

Michalis D. Mantzaris, Panagiotis K. Siogkas, Vassilis D. Tsakanikas, Vassiliki T. Potsika, Dimitrios S. Pleouras, Antonis I. Sakellarios, Georgios Karagiannis, George Galyfos, Fragiska Sigala, Nikolaos Liasis, Marija Jovanovic, Igor B. Koncar, Michael Kallmayer, and Dimitrios I. Fotiadis, *Fellow, IEEE*

***Abstract*—Carotid atherosclerotic plaque growth leads to the progressive luminal stenosis of the vessel, which may erode or rupture causing thromboembolism and cerebral infarction, manifested as stroke. Carotid atherosclerosis is considered the major cause of ischemic stroke in Europe and thus new imaging-based computational tools that can improve risk stratification and management of carotid artery disease patients are needed. In this work, we present a new computational approach for modeling atherosclerotic plaque progression in real patient-carotid lesions, with moderate to severe degree of stenosis (>50%). The model incorporates for the first time, the baseline 3D geometry of the plaque tissue components (e.g. Lipid Core) identified by MR imaging, in which the major biological processes of atherosclerosis are simulated in time. The simulated plaque tissue production results in the inward remodeling of the vessel wall promoting luminal stenosis which in turn predicts the region of the actual stenosis progression observed at the follow-up visit. The model aims to support clinical decision making, by identifying regions prone to plaque formation, predict carotid stenosis and plaque burden progression, and provide advice on the optimal time for patient follow-up screening.**

* This work has received funding from the European Union's Horizon 2020 research and innovation programme under grant agreement No 755320, as part of the TAXINOMISIS project.

D. I. Fotiadis is with the Unit of Medical Technology and Intelligent Information Systems, Department of Materials Science and Engineering, University of Ioannina, and with the Department of Biomedical Research, Institute of Molecular Biology and Biotechnology–FORTH, University Campus of Ioannina, 45110 Ioannina, Greece (phone: +30 26510 09006; email: fotiadis@uoi.gr).

M. D. Mantzaris, P. K. Siogkas, V. D. Tsakanikas, V. T. Potsika, and D. S. Pleouras are with the Unit of Medical Technology and Intelligent Information Systems, Department of Materials Science and Engineering University of Ioannina, Ioannina, Greece (e-mail: mdmantzaris@gmail.com, psiogkas4454@gmail.com, vasilistsakanikas@gmail.com, vpotsika@gmail.com, pleouras@live.com).

A. I. Sakellarios is with the Department of Biomedical Research, Institute of Molecular Biology and Biotechnology–FORTH, University Campus of Ioannina, Ioannina , Greece (e-mail: ansakel@cc.uoi.gr).

G. Galyfos and F. Sigala, are with the First Propedeutic Department of Surgery, National and Kapodistrian University of Athens, Athens, Greece (email: georgegalyfos@hotmail.com, drfsigala@yahoo.gr).

G. Karagiannis and N. Liassis are with Department of Vascular Diagnosis, AFFIDEA, Athens, Greece (email: gekaragiannis.gk@gmail.com, nikos.liasis@affidea.com).

Michael Kallmayer is with the Department for Vascular and Endovascular Surgery, Klinikum rechts der Isar, Technical University of Munich, Munich, Germany (email: Michael.Kallmayer@mri.tum.de).

I. B. Koncar and M. Macvanski are with the Department of Vascular and Endovascular Surgery, Faculty of Medicine, University of Belgrade, Belgrade, Serbia and with the Department of Vascular and Endovascular Surgery, Clinic Center of Serbia, Belgrade, Serbia (email: dr.koncar@gmail.com, macvanskimarija@yahoo.com).

I. Introduction

Stroke is the second most common cause of mortality in the EU, responsible for 440,000 deaths per year. It is a leading cause of disability in adults with more than 50 percent of stroke survivors becoming dependent on other people for their everyday activities. Stroke associated costs reach €45 billion per year, including direct and indirect costs for healthcare and productivity loss [1, 2].

In this context, carotid atherosclerotic plaque tissue growth is considered a major cause of ischaemic stroke events since enlarged plaques may erode or rupture leading to thromboembolism and cerebral infarction [2]. Of note, 10 to 15% of all strokes result from thromboembolism caused from a previously asymptomatic plaque of the internal carotid artery (ICA), with a degree of stenosis higher than 50% [2]. For this reason, new tools that can improve risk stratification and management of patients with moderate to severe carotid stenosis are needed.

To this end, several computational studies have been performed aiming to model the biological processes of atherosclerosis and simulate atherosclerotic plaque tissue progression in time [3-7]. However, the majority of these models are implemented in idealized two dimensional (2D) arterial geometries while only few studies are based on real human arterial geometries [6, 7]. Real human vessel geometries can be obtained by different cardiovascular imaging modalities including CT angiography, MR angiography and Intravascular Ultrasound (IVUS). Images can then be used for patient-specific (3D) reconstruction of the vessel's lumen and wall, and application of computational fluid dynamics (CFD) simulations. The calculated biomechanical forces including wall shear stress (WSS) distribution, are then used to simulate transendothelial infiltration of lipoproteins and inflammatory cells in the arterial wall that promote atherosclerotic plaque tissue growth. The mathematical formulation of the model is based on differential equations.

Herein, we present a novel computational approach for modeling atherosclerotic plaque progression in a real patient-carotid lesion, with moderate degree of stenosis (>50%). To this end, we use a previously validated model of plaque progression published by our group [7], and proceeded further by incorporating for the first time, the baseline 3D geometry of the plaque tissue components identified by MR imaging. The overall methodology and results are presented.

978-1-7281-1178-0/21/$31.00 ©2021 IEEE

II. MATERIALS AND METHODS

A. Cardiovascular MR image acquisition protocol

MRI examination was performed in a patient with >50% carotid stenosis using a 1.5-T whole-body system (Signa HDx, GE Healthcare, Waukesha, WI, USA) with a bilateral four-channel phased-array carotid coil (Machnet BV, Eelde, the Netherlands). Patient provided written informed consent and enrolled in the TAXINOMISIS clinical study (www.clinicaltrials.gov; ID: NCT03495830) protocol which was approved by the local competent ethics committee. The acquisition parameters for the MRI sequences were as follows: (i) TOF images: repetition time: 23 ms, effective echo time: 3.2 ms, field of view [FOV]: 160 mm, section thickness: 1 mm; (ii) fast-spin echo double-inversion recovery prepared sequences (T1W): repetition time: 1428.57 ms, effective echo time: 7.672 ms, FOV: 100 mm, section thickness: 3 mm; (iii) (T2W): repetition time: 1379.31 ms, effective echo time: 99.74 ms, FOV: 100 mm, section thickness: ≤ 2.5 mm (iv) (PDW): repetition time: 1379.31 ms, effective echo time: 7.67 ms, FOV: 100 mm, section thickness: ≤ 2.5 mm. The acquired data were stored in DICOM format.

B. Cardiovascular MR image analysis

Multicontrast MR image sequences TOF, T1W, T2W, and PDW were reviewed by two experienced radiologists (G.K. and M.J.) by consensus, using an in-house software implemented in MATLAB (The MathWorks, Natick, MA). Radiologists were blinded to patient clinical data. Luminal and outer wall boundaries were manually outlined at each slice location in TOF and T1W images respectively, while the presence or absence of plaque tissue components (e.g. fibrous tissue, lipid-rich necrotic core (LRNC), calcification or intraplaque hemorrhage (IPH)) were identified and manually annotated based on previously validated criteria [8].

C. 3D reconstruction of the carotid artery and plaque tissue components

The first step for the arterial 3D reconstruction is the registration of the annotated borders. For this process, the relative DICOM tags were utilized, in order to scale and rotate the different image series to a common plane. As T1W images are fewer in number than the TOF images, a linear interpolation algorithm is applied in order to fill in the "missing" frames. Afterwards, three different 3D models are created, following the same algorithmic process, which can be summarized in the next steps. (i) The borders from the annotation process are transformed to binary mask images, where the region inside the border is set to 1 and the region outside the border is set to 0. (ii) A volume is created by stacking all the relative masks. (iii) The 3D morhological snake model is applied to the 3D volumes, as presented in [9]. (iv) On the acquired 3D geometrical model, a re-meshing algorithm is applied (marching cubes) in order to refine the final surface meshed model. The 3 different models (lumen, outerwall and plaque tissue components) are registered to a common 3D arterial model.

D. Simulation of atherosclerotic plaque progression

Plaque growth simulation was performed by modeling the major biological processes of atherosclerosis (see, Fig.1) using several differential equations as previously described in detail [7]. In brief, the model performs a steady state simulation of luminal blood flow using the patient-specific blood velocity waveform obtained by Duplex Ultrasound. Blood flow simulation provides the WSS distribution required for the computation of the transendothelial flow rates. Patient-specific concentrations of LDL, HDL, and monocytes are utilized in a transient simulation to calculate their infiltration into the arterial wall in a WSS-dependent manner based on Kedem-Katchalsky equations (plasma flow, LDL, HDL) and available experimental data (monocyte transendothelial migration). Within the arterial wall, the main mechanisms of plaque formation are modelled based on the modified Navier-Stokes Equations (plasma flow) and the modified Convection-Diffusion-Reaction equations. In the arterial wall, LDL molecules are oxidized initiating an inflammatory response, while HDL levels mitigate this process by being competitively oxidized. Oxidized LDL particles further increase monocyte infiltration to the area by chemotaxis. Monocytes differentiate into macrophages which uptake oxidized LDL and are transformed to foam cells the cornerstone of plaque tissue formation. Macrophages secrete cytokines that promote contractile Smooth Muscle Cell (SMC) migration and differentiation from the media layer to the intima. Differentiated, synthetic SMCs produce collagen, a fibrotic tissue generating process that ultimately transforms atheromatus plaque to fibroatheromatic tissue. Lipid-laden foam cells (lipid core) and synthetic SMCs with collagen (fibrotic tissue) comprise the atherosclerotic plaque volume. The simulation was performed assuming a time period of 1 year. The resulted plaque density distribution is used to compute the volumetric strain which enables the simulation of the inward remodeling

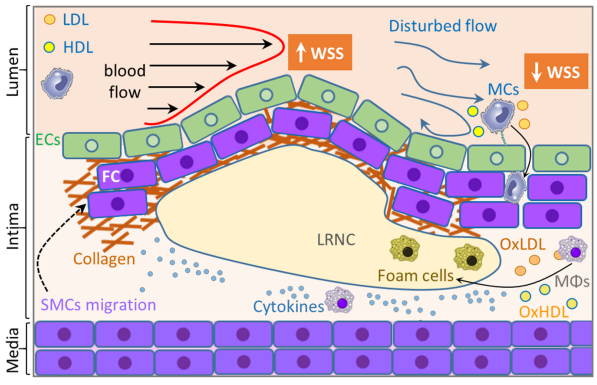

Figure 1. Major mechanisms of the atherosclerotic process modelled for plaque growth simulation. ECs; Endothelial Cells, MCs; Monocytes, MΦs; Macrophages, SMCs; Smooth Muscle Cells, FC; Fibrous Cap, OxLDL; Oxidized LDL-Cholesterol, OxHDL; Oxidized HDL-Cholesterol, LRNC; Lipid Rich Necrotic Core, WSS; Wall Shear Stress.

of the vascular wall (wall thickening). Initial plaque tissue components identified by cardiovascular MR imaging (i.e. Lipid Rich Necrotic Core) at baseline, are included in the model as impermeable structures while fibrous tissue is assumed as quiescent SMCs of the wall. The major plaque progression mechanisms simulated are depicted in Fig.1, while the material properties used for the inward remodeling of the wall are presented in Table I.

TABLE I. MATERIAL PROPERTIES USED FOR THE TISSUE COMPONENTS [10].

Parameter	Wall	Lipid
E_r(kPa)	10	1
E_θ(kPa)	100	1
$G_{r\theta}$(kPa)	50	1
$\nu_{r\theta}$	0.01	0.01
ν_{rz}	0.27	0.27

III. RESULTS

Fig. 2 illustrates the 3D reconstructed carotid artery of the patient, presenting a significant degree of luminal stenosis (>50%) in the ICA, upstream the bifurcation site. The reconstructed carotid geometry includes a Lipid Rich Necrotic Core (LRNC) identified by the two MRI specialists. Next, the steady state simulation of the luminal blood flow was performed and the WSS distribution is presented on the right panel. Importantly, a region with significantly low values of WSS (<1Pa) is located at the ICA, right next to the LRNC and downstream the carotid lesion.

In Fig. 3, the results of the plaque growth simulation are presented, for an assumed period of 1 year (left panel). Blood derived lipoproteins and monocytes infiltrate the vascular wall, in regions of low WSS (upper right panel) and their concentrations in turn, fuel a series of Convection-Diffusion-Reaction equations that ultimately result to new plaque tissue formation and plaque progression (middle right panel). The new plaque tissue accumulation deforms the vascular wall resulting in inward remodeling and luminal stenosis (lower right panel, inverted rainbow colouring). Importantly, low WSS values downstream the lesion are

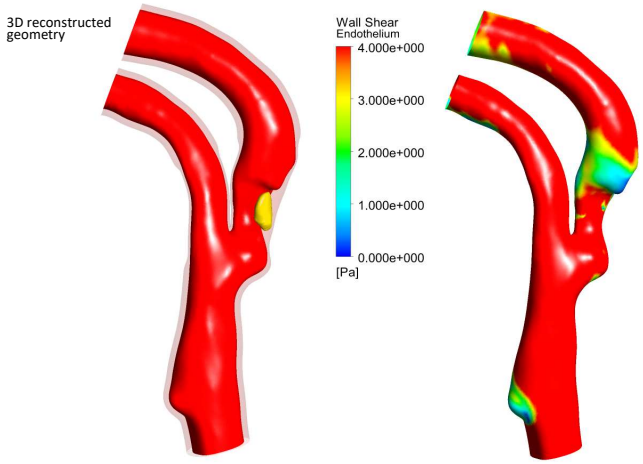

Figure 2. 3D reconstructed arterial geometry and WSS distribution of a real carotid bifurcation with a moderate degree of luminal stenosis (>50%) in the ICA, upstream the bifurcation site.

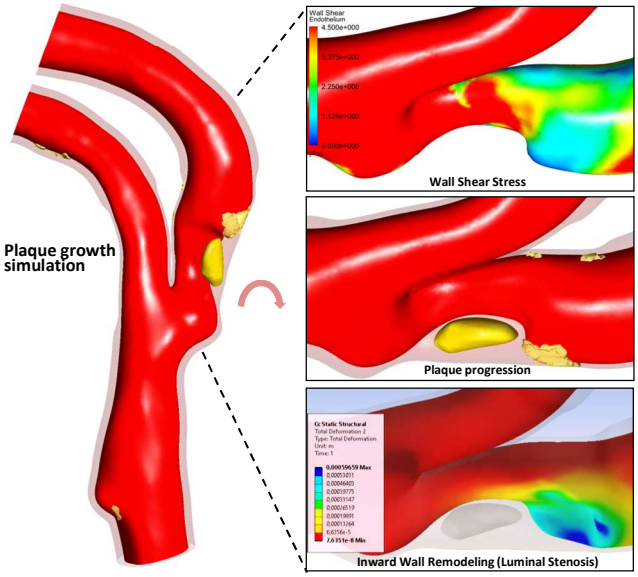

Figure 3. Simulation of atherosclerotic plaque progression in the ICA lesion with >50% stenosis. Lesion geometry and low WSS predict regions of future plaque progression and luminal stenosis.

associated with regions of plaque progression and luminal stenosis. Panels on the right are presented in a 90^0 degree angle matching Fig.1 perspective, for comparison.

Finally, the simulated luminal geometry is compared with the actual patient geometry, obtained at the 1 year follow-up visit (Fig. 4). Importantly, a progression of luminal stenosis is observed in the real follow-up artery at the downstream portion of the lesion (lower left panel) which is similar with the one predicted by the simulation (middle left panel) as compared with the baseline geometry (right panel).

IV. DISCUSSION

In this proof of concept study, we presented a new computational approach for the simulation of atherosclerotic plaque growth in a real patient carotid lesion with a moderate degree of stenosis (>50%). To the best of our knowledge, this is the first time in which baseline plaque tissue components, identified by multispectral MR imaging, are included in the initial 3D reconstructed artery providing in this way a more realistic, patient-specific plaque growth simulation. However, this first computational approach presents some limitations that are planned to be addressed in our future work. In particular, the presented plaque growth model simulates the major biological processes that lead to plaque tissue formation comprising lipid-laden foam cells and fibrous tissue. However, moderate (>50%) to severe (>70%) carotid stenotic lesions may also bear more complex compositions including calcifications and intraplaque hemorrhages that also affect plaque tissue stability [11]. In addition, recent elegant studies in the field of single-cell mapping of carotid atherosclerosis have pointed out the significant role of additional inflammatory cell populations in the course of asymptomatic and symptomatic carotid disease. These cells include CD4+ and CD8+ effector and cytotoxic T lymphocytes that comprise more than 50% of the total leukocyte population of the human carotid

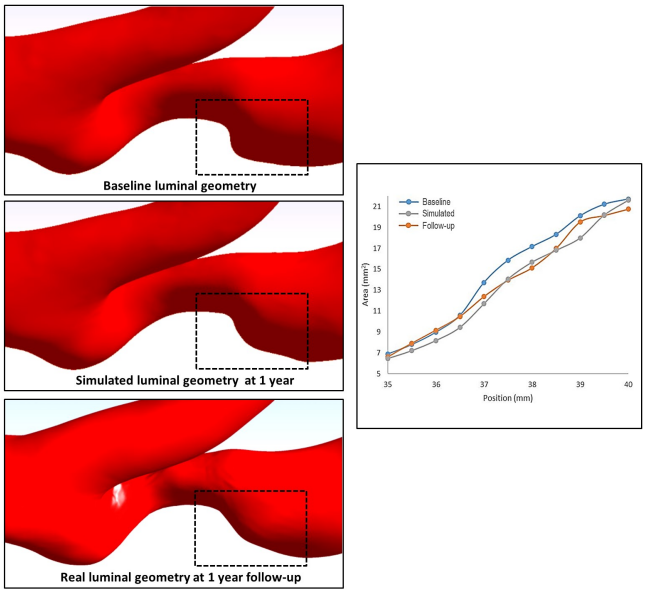

Figure 4. Comparison of the simulated luminal geometry with the actual patient luminal geometry at 1 year follow-up. Quantification of the luminal areas of the inset regions (left panels) are presented in the graph (right panel).

atherosclerotic plaque [12, 13]. Finally, a one-way interaction of the blood flow analysis, providing the baseline WSS distribution to the plaque growth simulation process, has been applied in the current study. However, progression of carotid lesions from moderate to severe stenosis may significantly alter blood flow and WSS dynamics during disease progression that need to be taken into account in the simulation process. Such refinements, including the incorporation in the model of T-cell populations and the biological processes involved in the formation of calcification and IPH as well as in fibrous cap thinning should help improve the current model and enhance its predictive accuracy and clinical utility. Model enrichment, refinement and validation are required and present the future aims of our work.

V. Conclusion

We present a new computational approach for modeling atherosclerotic plaque progression in real patient-carotid lesions, with moderate to severe degree of stenosis (>50%). The model incorporates for the first time, the baseline 3D geometry of the plaque tissue components identified by MR imaging. The simulated, newly synthesized plaque tissue results in the inward remodeling of the vessel wall promoting luminal stenosis which in turn predicts the actual stenosis observed at the follow-up visit. The model aims to improve risk stratification of carotid artery disease patients, by identifying regions prone to plaque formation, predict carotid stenosis and plaque burden progression, and provide advice on the optimal time for patient follow-up screening. Further enrichment and validation of the plaque growth model can provide clinicians with a tool to assist clinical decision making and management of carotid artery disease.

References

[1] H.A. Wafa, C.D.A Wolfe, E. Emmett, G.A Roth, C.O. Johnson, and Y. Wang, "Burden of Stroke in Europe: Thirty-Year Projections of Incidence, Prevalence, Deaths, and Disability-Adjusted Life Years," *Stroke,* vol. 51, Aug. 2020, pp. 2418-2427.

[2] A. R. Naylor, J. B. Ricco, G. J. de Borst, S. Debus, J. de Haro, A. Halliday, G. Hamilton, J. Kakisis, S. Kakkos, S. Lepidi, H. S. Markus, D. J. McCabe, J. Roy, H. Sillesen, J. C. van den Berg, F. Vermassen, C. Esvs Guidelines Committee, P. Kolh, N. Chakfe, R. J. Hinchliffe, I. Koncar, J. S. Lindholt, M. Vega de Ceniga, F. Verzini, R. Esvs Guideline Reviewers, J. Archie, S. Bellmunt, A. Chaudhuri, M. Koelemay, A. K. Lindahl, F. Padberg, and M. Venermo, "Editor's Choice - Management of Atherosclerotic Carotid and Vertebral Artery Disease: 2017 Clinical Practice Guidelines of the European Society for Vascular Surgery (ESVS)," *Eur J Vasc Endovasc Surg,* vol. 55, Jan. 2018, pp. 3-81.

[3] A. J. Brown, Z. Teng, P. C. Evans, J. H. Gillard, H. Samady, and M. R. Bennett, "Role of biomechanical forces in the natural history of coronary atherosclerosis," *Nat Rev Cardiol,* vol. 13, Apr. 2016, pp. 210-220.

[4] A. Parton, V. McGilligan, M. O'Kane, F. R. Baldrick, and S. Watterson, "Computational modelling of atherosclerosis," *Brief Bioinform*, vol. 17, Jul. 2016, pp. 562–575.

[5] N. A. Avgerinos, P. Neofytou, "Mathematical Modelling and Simulation of Atherosclerosis Formation and Progress: A Review," *Ann Biomed Eng,* vol. 47, Aug. 2019, pp. 1764-1785.

[6] A. I. Sakellarios, P. Bizopoulos, M. I. Papafaklis, L. Athanasiou, T. Exarchos, C. V. Bourantas, K. K. Naka, A. J. Patterson, V. E. L. Young, J. H. Gillard, O. Parodi, L. K. Michalis, and D. I. Fotiadis, "Natural History of Carotid Atherosclerosis in Relation to the Hemodynamic Environment," *Angiology*, vol. 68, Feb. 2017, pp. 109-118

[7] D. S. Pleouras, A. I. Sakellarios, P. Tsompou, V. Kigka, S. Kyriakidis, S. Rocchiccioli, D. Neglia, J. Knuuti, G. Pelosi, L. K. Michalis, and D. I. Fotiadis, "Simulation of atherosclerotic plaque growth using computational biomechanics and patient-specific data," *Sci Rep,* vol. 10, Oct. 2020 pp.17409.

[8] T. Saam, M.S. Ferguson, V.L. Yarnykh, N. Takaya, D. Xu, N.L. Polissar, T.S. Hatsukami, and C. Yuan, "Quantitative Evaluation of Carotid Plaque Composition by In Vivo MRI," *Arterioscler Thromb Vasc Biol*, vol. 25, Jan. 2005, pp. 234-239.

[9] P. Márquez-Neila, L. Baumela, and L. Alvarez, "A morphological approach to curvature-based evolution of curves and surfaces," *IEEE Trans Pattern Anal Mach Intell*, vol. 36, Jan. 2014, pp. 2-17.

[10] K. K. Wong, P. Thavornpattanapong, S.C. Cheung, Z. Sun, and J. Tu, "Effect of calcification on the mechanical stability of plaque based on a three-dimensional carotid bifurcation model," *BMC Cardiovasc Disord*, vol. 12, Feb. 2012, pp. 7.

[11] J. Pelisek, R. Hegenloh, S. Bauer, S. Metschl, J. Pauli, N. Glukha, A. Busch, B. Reutersberg, M. Kallmayer, M. Trenner, H. Wendorff, P. Tsantilas, S. Schmid, C. Knappich, C. Schaeffer, T. Stadlbauer, G. Biro, U. Wertern, F. Meisner, K. Stoklasa, A. Menges, O. Radu, S. Dallmann-Sieber, A. Karlas, E. Knipfer, C. Reeps, A. Zimmermann, L. Maegdefessel, and H. Eckstein, "Biobanking: Objectives, Requirements, and Future Challenges-Experiences from the Munich Vascular Biobank," *J Clin Med*, vol. 8, Feb. 2019, pp. 251.

[12] M. A. C. Depuydt, K. H. M. Prange, L. Slenders, T. Örd, D. Elbersen, A. Boltjes, S. C. A. de Jager, F. W. Asselbergs, G. J. de Borst, E. Aavik, T. Lönnberg, E. Lutgens, C. K. Glass, H. M. den Ruijter, M. U. Kaikkonen, I. Bot, B. Slütter, S. W. van der Laan, S. Yla-Herttuala, M. Mokry, J. Kuiper, M. P. J. de Winther, and G. Pasterkamp, "Microanatomy of the Human Atherosclerotic Plaque by Single-Cell Transcriptomics," *Circ Res*, vol. 127, Nov. 2020, pp. 1437-1455.

[13] D. M. Fernandez, A. H. Rahman, N. F. Fernandez, A. Chudnovskiy, E. D. Amir, L. Amadori, N. S. Khan, C. K. Wong, R. Shamailova, C. A. Hill, Z. Wang, R. Remark, J. R. Li, C. Pina, C. Faries, A. J. Awad, N. Moss, J. L. M. Bjorkegren, S. Kim-Schulze, S. Gnjatic, A. Ma'ayan, J. Mocco, P. Faries, M. Merad and C. Giannarelli, "Single-cell immune landscape of human atherosclerotic plaques," *Nat Med*, vol. 25, Oct. 2019, pp. 1576-1588.